Hindawi
Advances in Materials Science and Engineering
Volume 2017, Article ID 9523174, 7 pages
https://doi.org/10.1155/2017/9523174

Research Article

Study on the Effect of Different Fe_2O_3/ZrO_2 Ratio on the Properties of Silicate Glass Fibers

Jianxun Liu,[1,2] Jianping Yang,[2] Haibin Huo,[1] Liang Lei,[2] Ying Cui,[2] and Zhishen Wu[1,2]

[1] *International Institute for Urban Systems Engineering, Southeast University, Nanjing 210096, China*
[2] *National & Local Joint Engineering Research Center of "Basalt Fiber Production and Application", Southeast University, Nanjing 210096, China*

Correspondence should be addressed to Zhishen Wu; zswu@seu.edu.cn

Received 14 April 2017; Accepted 21 August 2017; Published 28 September 2017

Academic Editor: Belal F. Yousif

A series of silicate glass fibers with different ratios of Fe_2O_3/ZrO_2 were prepared, and their corrosion resistance, mass loss, and strength loss were characterized. The crystallization and melting properties of the fibers were analyzed by differential scanning calorimetry (DSC), high temperature viscometer, and high temperature microscope. The results show that the deformation temperature, sphere temperature, hemisphere temperature, and crystallization temperature of the fiber initially decrease and then increase with the increase of Fe_2O_3/ZrO_2 ratio, while the molding temperature decreases with the increase of the ratio of Fe_2O_3/ZrO_2. When the ratio is close to 1 : 1, its alkali resistance is almost same as that of AR-glass fiber, and the drawing process performance is better. However, with the increase of the ratio, its alkali resistance continues to decline and the poor wire drawing performance is not conducive to the drawing operation.

1. Introduction

Basalt fiber is a new kind of inorganic nonmetallic silicate fiber prepared by melt drawing process with natural basalt ores as raw materials [1, 2]. Compared with ordinary glass fiber, basalt fiber has excellent high tensile strength, elastic modulus, creep resistance, fatigue resistance, high temperature resistance, and other properties [3, 4] and is generally considered as a material with excellent alkali resistance [5–8], which could be widely used in many fields such as civil engineering, transportation, and marine engineering [9, 10].

Most silicate glass fiber is easily eroded by alkali in alkaline environment, such as ordinary alkali-free glass fiber and high strength glass fiber. In the 1970s the British Pilkington company invented alkali resistant glass fiber and improved the alkali resistance of fiber [11], which solved the problems of strength reduction, cracking, and leakage of the ordinary glass fiber due to the alkaline reaction with cement. However, the raw materials for alkali resistant glass fiber are very expensive, which limits its wide application.

By comparison of the components of basalt fiber and alkali resistant glass fiber, it can be concluded that the characteristic component of basalt fiber is Fe_2O_3 and the characteristic component of alkali resistant glass fiber is ZrO_2. Referring to the solubility product constant table, the solubility product constants of $Fe(OH)_3$ and $ZrO(OH)_2$ are 4.0×10^{-38} and 6.3×10^{-49}, respectively, which are both very small. Therefore, it can be also understood for the mechanism of alkali erosion that Fe_2O_3 on the fiber surface will be converted to $Fe(OH)_3$ jelly under the action of alkali solution and form a dense film on glass surface through dehydration polymerization, which can prevent the erosion to fiber from the alkali solution and hydrate. Similarly, when the alkali resistant glass fiber is in alkaline solution, ZrO_2 on the fiber surface will be converted to $ZrO(OH)_2$ jelly and form a dense film on glass surface to prevent the erosion [12].

The alkali resistant glass fiber contains ZrO_2 with absence of Fe_2O_3, while basalt fiber contains Fe_2O_3 without ZrO_2. In recent years, Lipatov et al. studied the influence of ZrO_2 on the alkali resistance, mechanical properties, and crystallization properties of basalt fiber [13, 14].

In this paper, based on the small solubility product constant of $Fe(OH)_3$ and $ZrO(OH)_2$ and the formation of a protective film on the glass fiber surface, silicate glass fibers

Table 1: Chemical composition of samples (wt%).

Component	1#	2#	3#	4#	E-glass	AR-glass
SiO_2	61.00	61.00	61.00	61.00	54.35	62
Al_2O_3	0.50	0.50	0.50	0.50	14.90	1.0
CaO	5.80	5.80	5.80	5.80	16.60	4
MgO	0.80	0.80	0.80	0.80	4.6	/
K_2O	2.50	2.50	2.50	2.50	0.15	3.0
Na_2O	13.00	13.00	13.00	13.00	0.15	11
TiO_2	1.00	1.00	1.00	1.00	0.49	5
ZrO_2	16.00	12.00	8.00	4.00	/	14
Fe_2O_3	0.20	4.20	8.20	12.20	0.21	/
B_2O_3	/	/	/	/	8.7	/

with different ratios of Fe_2O_3/ZrO_2 were prepared, and the effect of different Fe_2O_3/ZrO_2 ratio on alkali resistance fiber and its drawing process performance was investigated.

2. Experimental

2.1. Ingredient Formulae. As showed in Table 1, a composition scheme with various proportions of Fe_2O_3/ZrO_2 was designed in which the contents of SiO_2, Al_2O_3, CaO, MgO, K_2O, Na_2O, and TiO_2 kept unchanged. Basalt ore was used as main raw material, and quartz sand, zircon, industrial grade iron oxide, alumina, magnesium oxide, calcium oxide, sodium carbonate, and potassium carbonate were used as auxiliary raw material, among which zircon was used to introduce ZrO_2 while basalt ore and industrial iron were used to introduce Fe_2O_3.

2.2. Preparation Process. The raw materials were weighed according to Table 1, mixed uniformly, and melted in the home-made platinum crucible. Melting was kept at 1510 ± 10°C for 24 hours with continuous stirring to obtain a clarified and homogenized glass melt, which was then poured on to a heat resistant steel plate and cooled down to obtain a glass block as the samples. The samples were placed in a self-designed drawing crucible for wire drawing, and the sample fibers with required diameters were obtained by adjusting the temperature of the magma, the height of the liquid surface, and the speed of the wire drawing machine.

2.3. The Testing Process. The alkali resistance of glass samples was evaluated by two methods: mass loss and strength retention. The mass and strength of the samples before and after the alkali etching were measured by the electronic analytical balance (Shanghai JA1003) and the fiber tensile tester (Shanghai Institute of Applied Science and Technology, XQ-1A), respectively. And the mass loss rate was calculated according to (1) (M_1: mass of samples before etching with an alkaline solution; M_2: mass of samples after etching with an alkaline solution). The strength retention rate was calculated according to (2) (T_1: fiber strength before alkali solution erosion; T_2: fiber strength after alkali solution erosion).

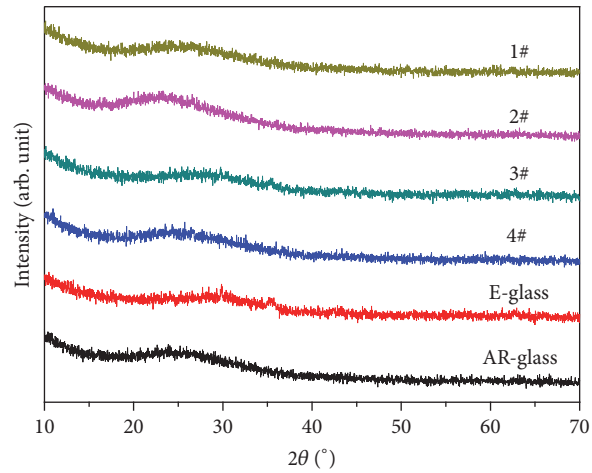

Figure 1: X-ray diffraction pattern of fiber samples.

$$\text{Mass loss rate } (\%) = \frac{M_1 - M_2}{M_1} \times 100 \quad (1)$$

$$\text{Strength retention rate } (\%) = 1 - \frac{T_1 - T_2}{T_1} \times 100. \quad (2)$$

The crystallization temperature of the glass samples was measured by a differential scanning calorimetry (DSC, DSC200F3Maia). The high temperature viscosity and melting properties of the glass samples were measured by high temperature rotational viscometer (Rheoteonic II) and high temperature microscope (OCA20LHT), respectively.

3. Results and Discussion

3.1. Effect of Fe_2O_3/ZrO_2 on Crystalline Phase of Samples. Silicate glass fiber is a product of high temperature melting and drawing. In order to investigate whether the process contains undamaged mineral phase or crystalline phase, the fiber was analyzed by X-ray diffraction, as shown in Figure 1.

Table 2: Mass and mass loss rate of samples before and after corrosion in NaOH solution.

Sample	1#	2#	3#	4#	E-glass	AR-glass
M_1/g	10.5452	10.5235	10.5134	10.5012	10.5418	10.5057
M_2/g	10.4693	10.4382	10.4083	10.3752	10.2761	10.4090
Mass loss rate/%	0.72	0.81	1.00	1.20	2.52	0.92

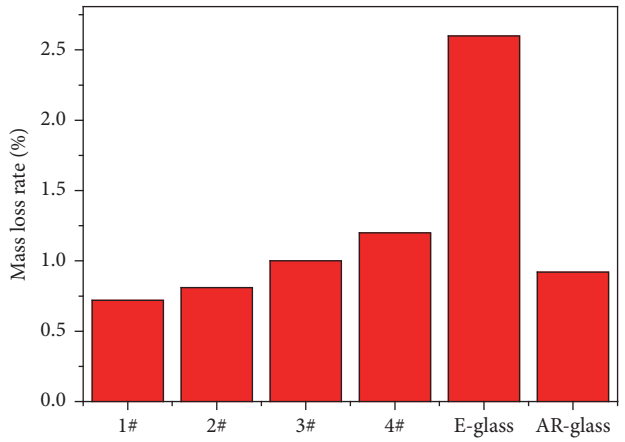

Figure 2: Mass loss rate of samples after corrosion in NaOH solution (unit: %).

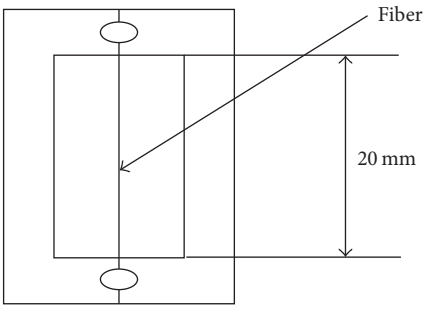

Figure 3: Tensile test specimen of fibers.

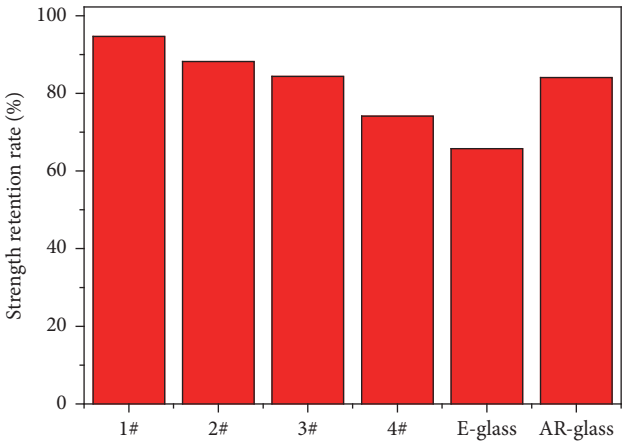

Figure 4: Strength retention rate of samples after corrosion in saturated $Ca(OH)_2$ solution.

Therefore, the fiber was analyzed by X-ray diffraction and was shown in Figure 1. It can be seen from Figure 1 that the X-ray diffraction pattern of the fiber has only steamed bread peaks similar to glass. This shows that silicate glass fibers do not have any mineral phases and crystalline phases and exist in the form of amorphous.

3.2. Effect of Fe_2O_3/ZrO_2 on Mass Loss Rate of Samples. The melted glass pieces were crushed and the granules were sieved through a 20–40 mesh sieve to obtain powder samples. Samples with known mass (M_1) were placed in a conical flask of 2 mol/L NaOH solution and then placed in a water bath at a constant temperature of 99 ± 0.5°C. The conical flasks were connected to a reflux condenser and sealed with plastic wrap. After 24 h, the powder was weighed again to obtain its mass (M_2), and the mass loss rate was calculated. The measured data were presented in Table 2, and the mass loss rate of each sample was shown in Figure 2.

The weight loss rate of 1# sample is the smallest, the weight loss rates of 1#~4# samples increase with the increase of Fe_2O_3/ZrO_2 ratio, and the weight loss rate of 3# is close to that of AR-glass indicating that their alkali resistances are almost equal. The weight loss rate of the E-glass without ZrO_2 and Fe_2O_3 is the highest, which indicates that the E-glass is most resistant to alkali attack.

3.3. Effect of Fe_2O_3/ZrO_2 on Strength Retention of Samples. Prepared fibers were immersed in $Ca(OH)_2$ saturated solution and heated at 99 ± 0.2°C for 4 h. The tensile strength of the fibers before and after etching was measured according to ASTMD3379-75. A single fiber was bonded to the board, as shown in Figure 3. The experiment was carried out by using the 100 cN sensor tensile tester and the testing speed was 2 mm/min. During the test, once the fiber was fixed by the instrument, both sides of the cardboard were cut off with the scissors. For each fiber sample, 25 effective strength values were recorded and then were averaged. The tensile strength retention rates are calculated and presented in Table 3. The trend of strength retention rate is shown in Figure 4.

It can be seen that the tensile strength of the 1# sample is the highest before the alkali etching, and the retention rate of the strength after the alkali erosion is the largest. The strength retention rates of 1#~4# samples decrease with the increase of the ratio of Fe_2O_3/ZrO_2, and the strength retention rate of 3# is most close to that of AR-glass fibers, indicating that the alkali resistance of the two samples is the same. E-glass fibers

Table 3: Tensile strength and strength retention rate of samples before and after corrosion in saturated $Ca(OH)_2$ solution.

Sample	1#	2#	3#	4#	E-glass	AR-glass
T_1/MPa	2936.72	2798.74	2240.21	1804.86	2340.27	2417.90
T_2/MPa	2780.49	2468.69	1889.44	1338.11	1538.56	2032.74
Strength retention rate/%	94.68	88.21	84.34	74.14	65.74	84.07

do not contain ZrO_2 and Fe_2O_3, so its strength retention rate is the lowest indicating the worst alkali resistance. Reference [13] mentions that the addition of less than 3.1 wt% ZrO_2 increases the alkali resistance of the basalt fibers by 37%. The addition of more than 3.1 wt% ZrO_2 to the glass batch reduces the alkali resistance and tensile strength of the basalt fibers. Compared with this paper, there are some differences in data. The reason may be that the chemical composition of the sample is different.

In summary, the addition of ZrO_2 in the glass could significantly improve the alkali resistance of the glass system, because the ZrO_2 on the glass surface will be converted into $ZrO(OH)_2$ jelly and form a layer of dense membrane on the glass surface by dehydration polymerization to make it more resistant to the corrosion of the alkali solution and other hydrides [12–17]. The mass loss rate and strength retention rate of the glass samples decrease with the increase of the ratio of Fe_2O_3/ZrO_2. It is worth noting that when the ratio of Fe_2O_3/ZrO_2 is close to 1:1 (3# sample), the mass loss rate and strength retention rate are almost the same as those of AR-glass. The results show that 3# and AR-glass have the similar ability to resist alkali corrosion. In glass system, Fe^{3+} exists in two states: $[FeO_4]$ and $[FeO_6]$ [18, 19]; when a monovalent alkali metal ions or divalent alkali metal ions exist, Fe^{3+} will form $[FeO_4]$ tetrahedron and get into the -Si-O-Si- network as a network connector, so that the structure of the glass becomes tighter. On the contrary when there are no monovalent alkali metal ions and divalent alkali metal ions or the ion concentration is low, Fe^{3+} would be in the glass network gap to form $[FeO_6]$ octahedron. At the same time, Fe^{3+} ions also have a certain accumulation effect on the oxygen ions in the $[SiO_4]$ tetrahedron, which makes the structure denser [20]. Both of them could prevent further corrosion of the alkali solution on the fiber surface and the stability of the vitreous structure will not be broken. The relevant research has been carried out by Hwang and Lim [21], and it is considered that the oxidation state of iron has the following dynamic equilibrium relation.

$$\text{Low temperature, strong alkalinity, oxidizability} \longrightarrow$$
$$Fe^{2+} \longleftrightarrow Fe^{3+} \quad (3)$$
$$\longleftarrow \text{High temperature, strong acidity, reducibility}$$

Because the pure FeO does not exist in nature, when the temperature reaches 1475°C, part of Fe_2O_3 would be broken down and release oxygen to form Fe^{2+}, so Fe^{2+} and Fe^{3+} will always coexist in the silicate glass and the ratio varies with the melting conditions.

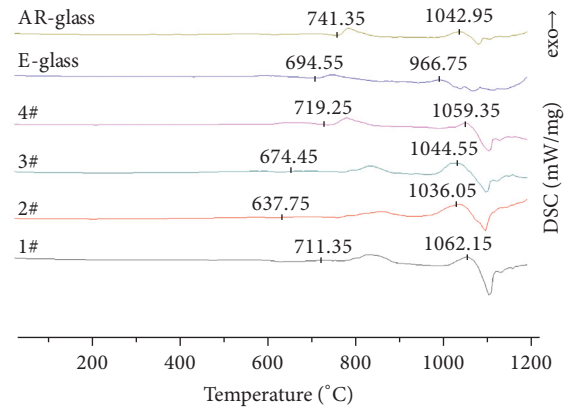

Figure 5: DSC curves of fibers.

An important structure of ferrous ferrite (Fe^{3+}-O-Fe^{2+}) forms, when Fe^{3+} and Fe^{2+} coexist in a silicate glass system. When Fe^{3+} ions in Fe^{3+}-O-Fe^{2+} structure are in tetrahedral coordination, they act as the network formers, while when Fe^{2+} ions are in octahedral coordination they are the network modifiers. When there are excess Fe^{3+} ions, the excess Fe^{3+} could only be in octahedral coordination network modifier position, and the formation of Si^{4+}-O-Fe^{3+} structure could make the fiber has tighter structure, better chemical stability, and better mechanical performance. On the other hand, when there are excess Fe^{2+} ions, the excess Fe^{2+} are also in octahedral coordination network modifier position, and the formation of Si^{4+}-O-Fe^{2+} structure could also prevent further erosion of the alkali solution on the fiber surface.

3.4. Effect of Fe_2O_3/ZrO_2 on Crystallization Behavior of Samples. The glass transition temperature (T_g) and the crystallization exothermic peak temperature (T_p) [22] of the glass samples were measured at the heating rate of 10°C/min in the high purity nitrogen atmosphere, which are shown in Table 4 and in Figure 5.

It could be seen that the glass transition temperature initially decreases from 711.35°C to 637.75°C and then rises to 719.25°C, and the crystallization exothermic peak temperature also decreases from 1062.15°C to 1036.05°C and then rises to 1059.35°C. These results indicate that T_g and T_p have a parabola-like trend with the increase of Fe_2O_3/ZrO_2. When the ratio of Fe_2O_3/ZrO_2 is close to 1:3, T_g and T_p reach the minimum values of 637.75°C and 1036.05°C respectively, and then T_g and T_p begin to rise again. When the ratio of Fe_2O_3/ZrO_2 is less than 1:3, the crystallization temperature of the glass samples is reduced, and the crystallization ability

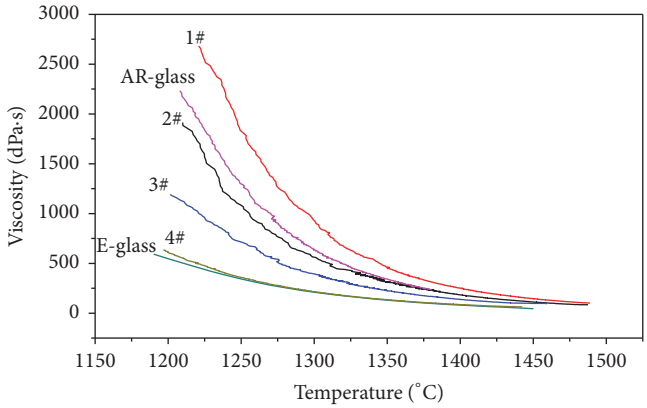

Figure 6: Viscosity-temperature curve of samples.

Table 4: Crystallization properties of samples.

Sample	T_g/°C	T_p/°C	$(T_p - T_g)$/°C
1#	711.35	1062.15	350.8
2#	637.75	1036.05	398.3
3#	674.45	1044.55	370.1
4#	719.25	1059.35	340.1
E-glass	694.55	966.75	272.2
AR-glass	741.35	1042.95	301.6

is improved. Furthermore, when the ratio of Fe_2O_3/ZrO_2 is more than 1 : 3, the crystallization temperature of glass samples begins to increase, and the crystallization ability is reduced. This is because Fe^{3+} is mainly present in the form of $[FeO_4]$ when Fe_2O_3 is initially added. Fe^{3+} has an internal polarization effect on the network frame of silicate glass, which makes the network connected tightly, the viscosity of silicate glass increased, and the crystallization ability enhanced. With the increase of the content of Fe^{3+}, Fe_2O_3 would be mainly $[FeO_6]$, manifesting as the increase of the external polarization, which results in gradually loosed network structure of silicate glass, the reduced viscosity, and the reduced crystallization ability. At the same time, T_p of 3# and AR-glass are not significantly different, while T_g of 3# is significantly lower than that of the AR-glass. Therefore, liquid phase is easier to form in the 3# sample during the melting process which can reduce energy consumption. Reference [13] mentions that when the content of ZrO_2 increases from 0 to 6.9 wt%, T_p increases from 940°C to 1005°C. The results show that T_p and T_g increase with the increase of ZrO_2 content. The results of this study are consistent with our study.

3.5. Effect of Fe_2O_3/ZrO_2 on High Temperature Viscosity of Samples. The high temperature viscosity of glass samples was tested. The viscosity-temperature curve is shown in Figure 6, and the corresponding temperature for the samples at $\log \eta = 2.5$ is shown in Table 5.

Considering the inclinations of the curves in Figure 4, the viscosity of 1# has the largest changing trend as the temperature decreases, followed by 2#, 3#, and 4# successively. The viscosity-temperature curve of E-glass is smooth and the viscosity is small. The trends of viscosity curves of AR-glass and 1# samples are basically the same, which might be due to the similar ZrO_2 content of 1# and AR-glass. ZrO_2 is octahedral coordination ($N = 8$), and the radius of Zr^{4+} is large. Under the same electric charge condition, with the increase of the coordination number (N) of the cation in the glass melt, the accumulation of silicon oxygen groups is enhanced and then the viscosity increases. Therefore, the viscosity of 1# and AR-glass is relatively larger. The viscosity of 3# is significantly better than that of AR-glass, which could meet the test results of crystallization properties of glass samples.

Table 5: Molding temperature of the samples (unit: C).

Sample	$\log \eta = 2.5$
1#	1379.23
2#	1348.55
3#	1318.9
4#	1260.54
E-glass	1256.67
AR-glass	1356.71

As shown in Table 5, with the increase of the ratio of Fe_2O_3/ZrO_2 in the glass samples, the corresponding temperature of $\log \eta = 2.5$ decreases, which is the drawing molding temperature. At this time, the drawing molding temperature of 3# is obviously lower than that of AR-glass, which could be beneficial to energy saving and production cost reduction.

3.6. Effect of Fe_2O_3/ZrO_2 on High Temperature Melting of Samples. The glass samples were placed in a furnace and heated up at a rate of 10°C/min. The deformation temperature (DT), sphere temperature (ST), and hemisphere temperature (HT) of the glass samples are plotted in Figure 7. The melting states of the glass samples at different temperatures are shown in Figure 8.

From Figure 8, it could be seen that the DT, ST, and HT of the glass samples initially decrease and then increase with the increase of Fe_2O_3/ZrO_2, and the change trend is presented in Figure 5. When the ratio of Fe_2O_3/ZrO_2 is close to 1 : 1, the DT, ST, and HT decline to the lowest temperature. Therefore, the melting temperature of 3# is the lowest. Compared with AR-glass, 3# has lower melting temperature, which is accordant with the results of high temperature viscosity test.

When the Fe_2O_3 content in the glass samples increases, the ZrO_2 content will decrease, which results in the change trend of the melting temperature of 1#~4# samples. Zr^{4+} is present in the form of $[ZrO_6]$ octahedral in the zirconium silicate melts. There are at least two silicon oxygen tetrahedrons between Zr^{4+} ions, and the bond strength of Zr-O-Si bond is high and is not readily destroyed at higher temperature. As a result, the melting temperatures of 1# and AR-glass are higher, while the melting temperatures of 2#, 3#, and 4# decrease with the decrease of ZrO_2 content (increasing

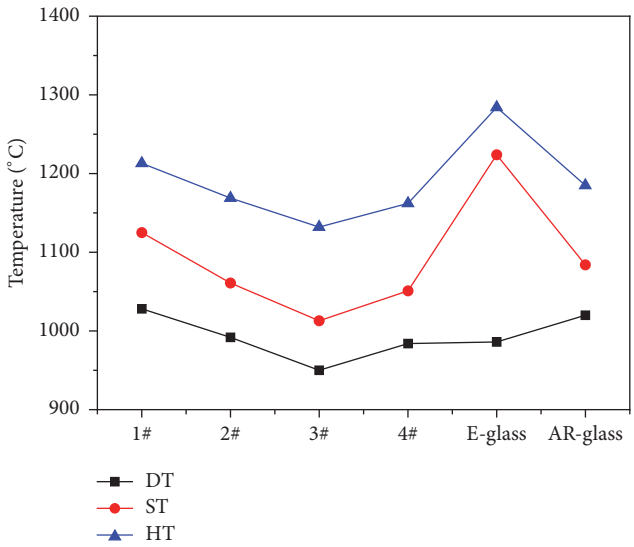

Figure 7: Melting temperature curve of samples.

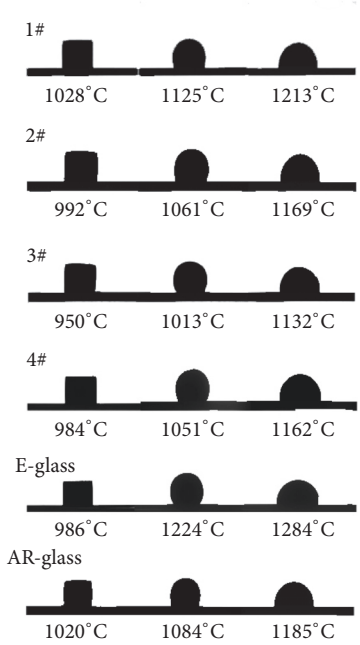

Figure 8: Melting state of samples.

ratio of Fe_2O_3/ZrO_2). At the same time, with the decrease of ZrO_2 content it is also accompanied by the increase of Fe_2O_3 content. Fe^{3+} is mainly present in the form of $[FeO_4]$ when Fe_2O_3 is added initially. Fe^{3+} has an internal polarization effect on the network frame of silicate glass, which makes the network connected tightly, so that the melting temperatures of 1# and AR-glass are higher. With the increasing content of Fe^{3+}, Fe_2O_3 would be mainly in the form of $[FeO_6]$, which manifests as the increase of the external polarization, results in the gradually loosed network structure of silicate glass, and further causes the decrease of the melting temperature.

4. Conclusions

(1) With the increase of Fe_2O_3/ZrO_2 ratio, the alkali resistance of silicate glass fiber decreases. When the ratio of Fe_2O_3/ZrO_2 is close to 1 : 1, the alkali resistances of 3# and AR-glass are almost same and are much higher than that of E-glass.

(2) With the increase of Fe_2O_3/ZrO_2 ratio, the crystallization temperature of silicate glass shows a trend of decreasing first and then increasing. When the ratio of Fe_2O_3/ZrO_2 is close to 1 : 1, T_p of 3# and AR-glass are almost same, while T_g is significantly lower than that of AR-glass. Therefore, the 3# has better crystallization properties compared with AR-glass.

(3) With the increase of Fe_2O_3/ZrO_2 ratio, the viscosities of 1# and AR-glass are the highest, and the viscosities of 2#, 3#, 4#, and E-glass decrease in sequence. When the ratio of Fe_2O_3/ZrO_2 is close to 1 : 1, 3# has lower viscosity and drawing molding temperature compared with AR-glass, and the wire drawing is easier in the process of fiber preparation.

(4) With the increase of Fe_2O_3/ZrO_2 ratio, the DT, ST, and HT of silicate glass initially decrease and then increase. When the ratio of Fe_2O_3/ZrO_2 is close to 1 : 1, the DT, ST, and HT of 3# have the lowest values, and 3# sample has a lower melting temperature compared with AR-glass, which could save energy consumption and reduce the production cost.

(5) If Fe_2O_3 is used to replace a part of ZrO_2, the AR-glass fiber still has good melting characteristics, chemical corrosion resistance, and mechanical properties, which could greatly reduce the production cost of AR-glass fiber.

Conflicts of Interest

The authors declare that they have no conflicts of interest.

Acknowledgments

The authors gratefully acknowledge the financial support provided by the Nature Science Foundation of Jiangsu Province, China (Grant no. BK20130623), and Production and School Joint Research Innovation Fund in Jiangsu Province, China (Grant no. BY2013079).

References

[1] K. J. Huang and M. Deng, "Stability of basalt fibers in alkaline solution and its effect on the mechanical property of concrete," *Acta Materiae Compositae Sinica*, vol. 27, pp. 150–154, 2010.

[2] Y. V. Lipatov, S. I. Gutnikov, M. S. Manylov, E. S. Zhukovskaya, and B. I. Lazoryak, "High alkali-resistant basalt fiber for reinforcing concrete," *Materials and Design*, vol. 73, pp. 60–66, 2015.

[3] Z. Li, T. Xiao, Q. Pan, J. Cheng, and S. Zhao, "Corrosion behaviour and mechanism of basalt fibres in acidic and alkaline environments," *Corrosion Science*, vol. 110, pp. 15–22, 2016.

[4] F. Z. Li, G. C. Li, H. M. Wang, and Q. Tong, "Effect of acid/alkali corrosion on properties of basalt fiber yarn," *Materials Review*, vol. 29, pp. 110–113, 2015.

[5] M. C. Wang, Z. G. Zhang, Z. J. Sun, and M. Li, "Corrosion resistance characteristic of continuous basalt fiber and its reinforcing composites," *Journal of Beijing University of Aeronautics and Astronautics*, vol. 32, no. 10, pp. 1255–1258, 2006.

[6] W. J. Huo, Z. G. Zhang, M. C. Wang, Z. J. Sun, and M. Li, "Experimental study on acid and alkali resistance of basalt fiber used for composites," *Acta Materiae Compositae Sinica*, vol. 24, pp. 77–82, 2008.

[7] X. Zhao, X. Wang, Z. S. Wu, and Z. G. Zhu, "Fatigue behavior and failure mechanism of basalt FRP composites under long-term cyclic loads," *International Journal of Fatigue*, vol. 88, pp. 58–67, 2016.

[8] B. Wei, H. Cao, and S. Song, "Tensile behavior contrast of basalt and glass fibers after chemical treatment," *Materials and Design*, vol. 31, no. 9, pp. 4244–4250, 2010.

[9] Y. H. Cui, "Primary properties of basalt continuous filament," *Journal of Textile Research*, vol. 26, pp. 120-121, 2005.

[10] V. Fiore, T. Scalici, G. D. Bella, and A. Valenza, "A review on basalt fibre and its composites," *Composites Part B: Engineering*, vol. 74, pp. 74–94, 2015.

[11] D. H. Qi, S. B. Qi, X. Q. Liu, and H. K. Wang, "Study on the application of high zirconia AR glass fiber," *Fiber Glass*, vol. 5, pp. 28–33, 2015.

[12] F. M. Li, "Application of glass fiber-reinforced concrete to engineerings," *Engineering Journal of Wuhan University*, supplement 1, pp. 504–506, 2007.

[13] Y. V. Lipatov, S. I. Gutnikov, M. S. Manylov, and B. I. Lazoryak, "Effect of ZrO2 on the alkali resistance and mechanical properties of basalt fibers," *Inorganic Materials*, vol. 48, no. 7, pp. 751–756, 2012.

[14] Y. V. Lipatov, I. V. Arkhangelsky, A. V. Dunaev, S. I. Gutnikov, M. S. Manylov, and B. I. Lazoryak, "Crystallization of zirconia doped basalt fibers," *Thermochimica Acta*, vol. 575, pp. 238–243, 2014.

[15] Y. K. Wu, F. H. Gong, and D. R. Sha, "Study of alkali resistance of fiber glass," *Fiber Glass*, vol. 4, pp. 6–14, 2004.

[16] M. C. Yang, M. L. Jiang, H. Zhang, and L. H. Shen, "Study on mechanism of zirconium containing alkali resistant glass fiber," *Journal of the Chinese Ceramic Society*, vol. 15, pp. 61–68, 1987.

[17] M. Ryoo, "New alkali resistant glass and alkali resistant mechanism," *Fiber Glass*, vol. 2, pp. 37–42, 1982.

[18] C. R. Kurkjian and E. A. Sigety, "Coordination of the ferric ion in glass," *Physics and Chemistry of Glasses*, vol. 9, pp. 73–83, 1968.

[19] R. A. Levy, C. H. P. Lupis, and P. A. Flinn, "Mössbauer analysis of the valence and coordination of iron cations in SiO_2-Na_2O-CaO glasses," *Physics and Chemistry of Glasses*, vol. 17, pp. 94–103, 1976.

[20] Y. F. Xia, R. C. Liu, S. X. Wang, C. Xu, S. Y. Pan, and Y. B. Cheng, "An investigation on coagulation effect of Fe^{3+} to oxygen ions in glasses," *Acta Physica Sinica—Chinese Edition*, vol. 34, pp. 259–262, 1985.

[21] K. Hwang and Y. Lim, "Chemical and structural changes of hydroxyapatite films by using a sol-gel method," *Surface and Coatings Technology*, vol. 115, no. 2-3, pp. 172–175, 1999.

[22] Q. H. Yang and Z. A. Jiang, "Study on the kinetics of crystallization of glass," *Journal of the Chinese Ceramic Society*, vol. 5, pp. 419–426, 1994.